Journal of Advanced Veterinary Research

https://advetresearch.com

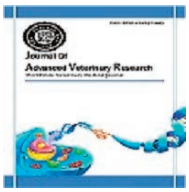

Ultrastructure of Ovarian Follicles and Testis in Zebra-snout Seahorse *Hippocampus barbouri* (Jordan & Richardson, 1908) under Aquaculture Conditions

Sinlapachai Senarat[1], Pisit Poolprasert[2], Jes Kettratad[3,4], Woranop Sukparangsi[5], Sansareeya Wangkulangkul[6], Gen Kaneko[7], Wannee Jiraungkoorskul[8*]

[1]*Department of Marine Science and Environment, Faculty of Science and Fisheries Technology, Rajamangala University of Technology Srivijaya, Trang 92150, Thailand.*
[2]*Program of Biology, Faculty of Science and Technology, Pibulsongkram Rajabhat University, Phitsanulok 65000, Thailand.*
[3]*Department of Marine Science, Faculty of Science, Chulalongkorn University, Bangkok 10330, Thailand.*
[4]*Marine Ecology and Marine Resources Utilization Research Unit, Aquatic Resources Research Institute, Chulalongkorn University, Bangkok 10330, Thailand.*
[5]*Department of Biology, Faculty of Science, Burapha University, Chon Buri 20131, Thailand.*
[6]*Department of Biology, Faculty of Science, Prince of Songkla University, Songkhla 90110, Thailand.*
[7]*School of Arts and Sciences, University of Houston-Victoria, 3007 N. Ben Wilson St. Victoria, Texas 77901, USA.*
[8]*Department of Pathobiology, Faculty of Science, Mahidol University, Bangkok 10400, Thailand.*

ARTICLE INFO

Original Research

Received:
30 November 2020

Accepted:
04 January 2021

Keywords:

Aquaculture, Gonad, Reproduction, Seahorse, Ultrastructure

ABSTRACT

The zebra-snout seahorse, *Hippocampus barbouri*, is an economically important marine fish and a potential candidate for aquaculture in Thailand. However, the reproductive ultrastructure of this seahorse is still poorly known. Transmission Electron Microscope (TEM) was used to characterize cellular morphology and ultrastructure of gametogenic stages in both sexes of *H. barbouri*. Based on morphology of the nucleus and unique characteristics of cytoplasmic organelles, oocytes in the oogenesis process of *H. barbouri* was classified into three distinct phases: primary growth phase (PG), secondary growth phase (SG) and atretic oocyte phase (AO). The early PG oocytes contained multiple nucleoli in close proximity to the nuclear membrane, showing the formation of cortical alveoli. The cytoplasm of late PG oocytes contained two distinctive cellular structures including lipid droplets and cortical alveoli and was enriched in rough endoplasmic reticulum, ribosome and mitochondria. The follicular complex complelety covered the oocyte at this phase and was classified into four distinct layers including zona pellucida, granulosa cells, basement membrane and theca cells. The yolk-granule formation was firstly observed in the early SG oocytes with well-developed microvilli in the zona pellucida and granulosa cells. During the late SG, the single-layered zona pellucida and the granulosa cells were well-organized. The dilated smooth endoplasmic reticulum and mitochondria were clearly visible in the granulosa cells. The AO oocytes exhibited disorganization of follicular complex. In male *H. barbouri*, spermatogonia and Sertoli-like cells occupied periphery of the germinal epithelium; however, the spermatocytes and spermatozoa were not observed in the germinal epithelium, possibly due to unique testis characteristics at this stage, season of the samples or aquaculture conditions. Taken together, this study unraveled characteristics of sexual differentiation in the zebra-snout seahorse and would provide benefit to monitor reproductive success of seahorse under aquaculture.

Introduction

Gametogenesis of syngnathids (Teleosts in family Syngnathidae, e.g. pipefish, seahorse, seadragon) has been rarely shown using histological and ultrastructural techniques, for example the spermatogenesis of *Hippocampus guttulatus* (Pirast *et al.*, 2015) and the ovarian ultrastructure showing the oogenetic classification of *H. erectus* (Wallace and Selman, 1990; Selman *et al.*, 1991). In general, similar to other vertebrate follicle morphology, the ovarian follicles architecture in

*Corresponding author: Wannee Jiraungkoorskul
E-mail address: wannee.jir@mahidol.ac.th

teleosts are constituted of four layers distinguished by histological techniques including the non-cellular zona pellucida enclosing an oocyte, granulosa cells, non-cellular basement membrane and theca cells covering periphery of the follicles (Grier, 2012; Senarat *et al.*, 2017). Shackley and King (1977) proposed that the oocyte growth is associated with the activity of granulosa cells and thecal cells. Using biochemical and ultrastructural approaches, indeed, granulosa cells and thecal cells in the ovarian follicles are capable of producing ovarian steroid hormones and thus these cells are essential to control of fish reproduction (Nagahama *et al.*, 1982; Fostier *et al.*, 1983; Senarat *et al.*, 2017). These roles of follicular cells and hormone production seems universal to several orders of fish, as shown in Labriformes (Santos-Silva *et al.*, 2015), Perciformes

ISSN: 2090-6277/2090-6269/

(Grier *et al*., 2017), Siluriformes (Rodrigues-Filho *et al*., 2017) and Scombriformes (Nyuji *et al*., 2013; Senarat *et al*., 2017).

The zebra-snout seahorse, *H. barbouri* Jordan & Richardson, 1908 (Syngnathiformes: Syngnathidae) is a coastal seahorse species of great economic importance. Wild capture of this seahorse species is permitted for both adults and juveniles, and individuals are currently exported for aquariums, ornamental fish stores and the production of biological medicine, especially traditional Chinese medicine for healthcare (Vincent, 1996; IUCN, 2002). Therefore, conservation programs are required to protect the zebra-snout seahorses in several measures including the restoration of its marine habitats and importantly the development of aquaculture to increase seahorse population. In this regard, the Phuket Marine Biological Center has played significant roles in developing aquaculture system for *H. barbouri* in Thailand since it was established in 2011. Complete cost-benefit analyses was conducted for brood stock maintenance, and scientific databases were established to overcome challenges regarding the risk of health status/lifestyle, nutritional requirement, gonadal differentiation and reproductive histology of this species (Kamnurdnin, 2017). Understanding gametogenesis of this seahorse will provide significant advantages over current aquaculture systems, by improving the seahorse reproduction under captive conditions. This study was aimed to elucidate the gametogenesis of *H. barbourin* using transmission electron microscopy with particular attention to ovarian folliculogenesis.

Materials and methods

Seahorses (*H. barbouri*) were reared in standard aquaculture system by using filtered seawater mechanically circulated from the natural resource at Phuket Marine Biological Center, Phuket Province, Thailand. The specimens were received during October to December 2017, and the specimens were also analyzed and described in Kamnurdnin (2017) for other histological observation. The samples were received as fixed and fresh tissues. Gonadal tissues of the seahorses at 30-31 days after birth (DAB) (n=6, 55.05±2.53 mm of total length) were fixed with 2.5% glutaraldehyde (in 0.1 M phosphate buffer, pH 7.4) at room temperature overnight and stored in the fixation solution. To prepare sample for transmission electron microscope (TEM) observation, the samples (n=3) were then treated with in 1% osmium tetroxide. Afterwards, they were processed using standard ultrastructural techniques (Rowden and Lewis, 1974). The thicknesses of 0.5 µm thick semi-thin Epon (glycid ether)-sections were directly stained with toluidine blue and observed for gonadal localization and determination of the sex using the light microscope with the digital camera (Leica 750). Ultrathin sections (about 90 nm thickness) were cut, placed on grids, stained in combination with uranyl acetate and lead citrate and examined using a transmission electron microscopy (TEM-2100 at 200kV).

The fresh gonadal tissues (n=3) were used to prepare frozen sections about 10 µm thicknesses. The sections were stained with Oil Red O (Culling, 1974) to visualize lipid distribution pattern. The section photos were taken using a light microscope equipped with a digital camera (Leica 750, Germany).

The experimental protocol was approved by the Animal Care and Use Committee of Faculty of Science in accordance with the guide for the care and use of laboratory animal prepared by Chulalongkorn University (Protocol Review No. 1623004).

Results

Sex determination in aquaculture seahorse H. barbouri using ultrastructure observation

To determine sex of seahorse, ultrastructure of the gonadal tissues was visualized by TEM. In this study, unique gonad structure of male/female seahorses was easily observed similar to other typical syngnatid. It revealed that gonadal tissues of the aquaculture seahorses contained oocytes at several developmental stages including oocytes in the primary growth phase (PG), secondary growth phase (SG) and atretic

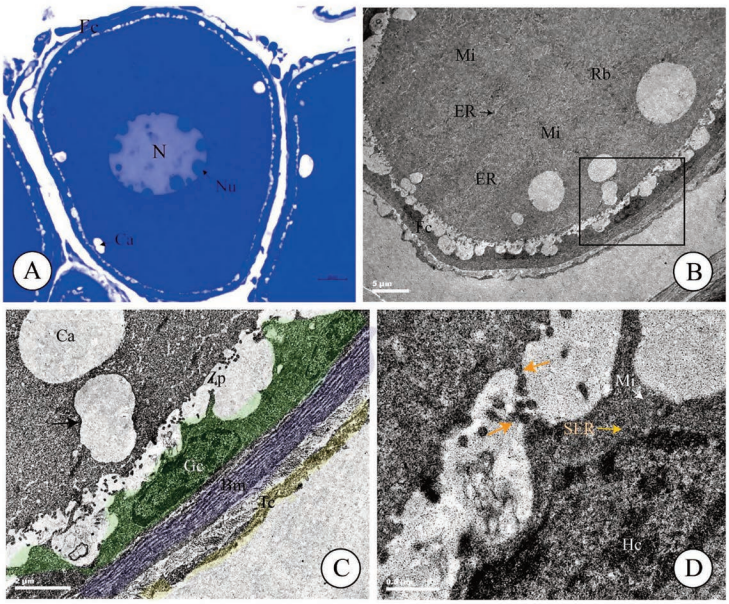

Fig. 1. Light microscope (A) and electron microscope (B-D) images of primary growth phase (PG) oocytes of *Hippocampus barbouri*. A: The oval-shaped early PG oocytes with a centrally-located spherical nucleus (N) was surrounded by the follicular complex (Fc). Several nucleoli (Nu) lined along the nucleus. The onset of cortical alveoli (Ca) was noted during this stage. B: Prominently developed organelles including mitochondria (Mi), endoplasmic reticulum (ER) and ribosome (Rb) were found in the cytoplasm. C-D: High magnification images showing the follicular complex composed of four distinct layers from outside to inside including theca cells (Tc), basement membrane (Bm), granulosa cells (Gc) and zona pellucida (Zp). The smooth endoplasmic reticulum (SER) and small mitochondria (Mi) of granulosa cell were observed. Microvilli (orange arrow) extended to the zona pellucida. Abbreviations: Black arrow = filled lipids, Hc = heterochromatin.

oocyte phase (AO) were observed (Figs. 1-5). However, the gonads from the reared seahorses in this study lacked the oogonium although several sections were examined. In addition, male characteristic in the gonad can be observed and evidenced by the presence of testicular parenchyma. Nevertheless, the mature spermatozoa of with developing flagellated morphology was not found in the gonads in this study (Fig. 6). Distinctive characters of the developing oocytes and cells in the testicular parenchyma are described below.

Ultrastructure of oocyte and follicular complex in primary growth phase (PG)

Based on the nucleus and cytoplasmic features, oocytes in primary growth phase (PG) were further classified into two stages including the early PG and late PG (Figs. 1-2). At the onset of the early PG development, oocytes were 35.50±1.09 µm in diameter, and the formation of cortical alveoli was observed close to the follicular complex (Fig. 1A). The oocytes had an oval shape and the moderately electron-dense, smooth, non-membrane bound surface (Fig. 1B). Small amounts of granular materials, mitochondria (Mi) and endoplasmic reticulum (ER) were present in the ooplasm (Fig. 1B).

The follicular complex had three layers including the innermost vitelline envelope, the granulosa cells and theca cells enclosing the follicular complex (Fig. 1C). A higher magnification electron micrograph identified the non-cellular and proteinaceous zona pellucida as an electron dense structure (Fig. 1C), whereas the granulosa cells were found to be the elongated-flatten cells surrounding an oocyte. Small mitochondria and smooth ER were observed in the granulosa cells (Fig. 1D). Microvilli were present intruding into the zona pellucida, which originally extended from the granulosa cells (Fig. 1D). Several clumped heterochromatins were present in the nucleoplasm of the granulosa cells (Fig. 1D). A distinct thin basement membrane was found as a barrier separating the granulosa cells from the layers of theca cells (Fig. 1C). A thin squamous layer

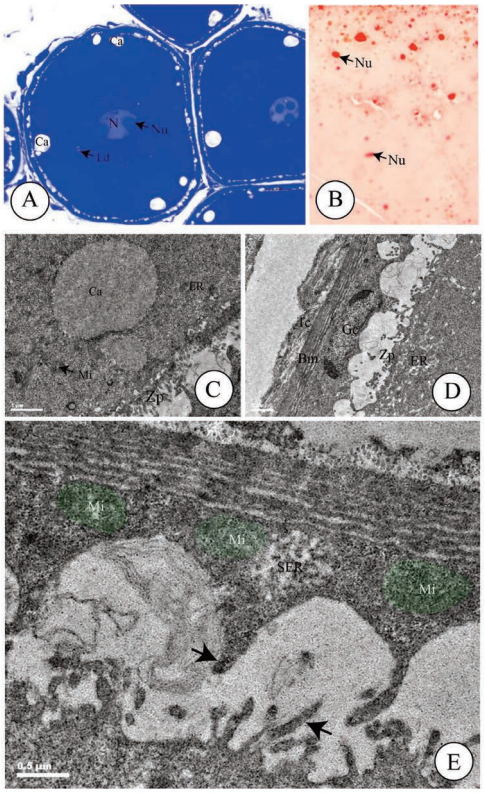

Fig. 2. Light microscope (A) and electron microscope (C-E) of primary growth phase (PG) oocytes of *Hippocampus barbouri*. A-B: Small lipid droplets (Ld) were found in the late PG near the nuclear membrane of nucleus (N). These droplets were conformed to Oil red O staining, as orange colour. C-D: The oval-shaped cortical alveoli (Ca) were developed near mitochondria (Mi) and endoplasmic reticulum (ER). The follicular complex was clearly observed with four layers [zona pellucida (Zp), granulosa cell (Gc), basement membrane (Bm) and theca cell (Tc)]. E: A high magnification image showing mitochondria (Mi) and smooth endoplasmic reticulum (SER) of the granulosa cells together with the well-developed microvilli (arrows) in the zona pellucida. Abbreviation: Nu = nucleoli

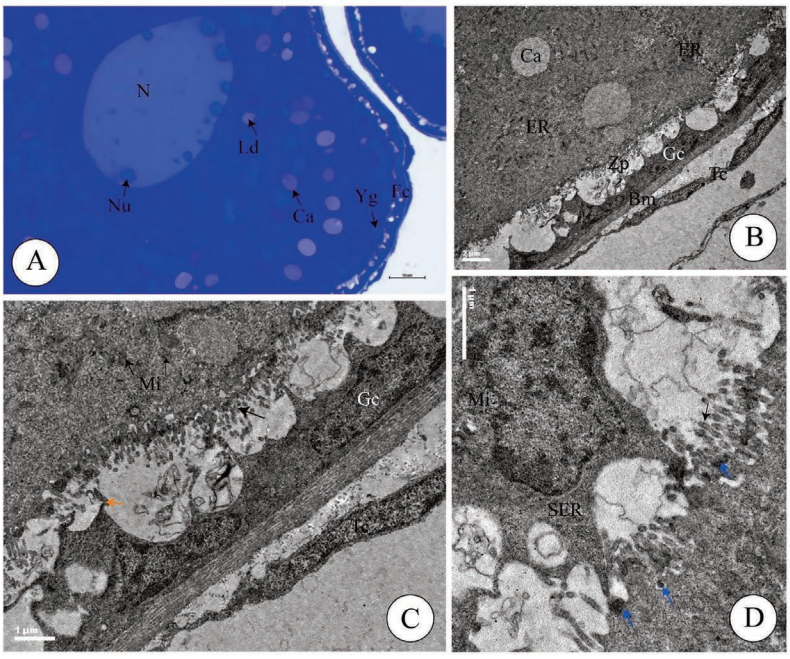

Fig. 3. Light microscope (A) and electron microscope (B-D) images of early secondary growth step oocytes of *Hippocampus barbouri*. A: Small yolk granules (Yg) was first formed close to the follicular complex (Fc). B-C: The well-developed endoplasmic reticulum (ER) and mitochondria (Mi) were observed in the ooplasm near the follicular complex with four distinct layers [zona pellucida (Zp), granulosa cell (Gc), basement membrane (Bm) and theca cell (Tc)]. The cytoplasmic extension (orange arrow) formed in the granulosa cells penetrated to the zona pellucida (black arrow) D: A high magnification image showing the granulosa cells containing the well-developed mitochondria (Mi) and smooth endoplasmic reticulum (SER). The microvilli (arrow) was found to be prominent. Note the formation of small electron dense masses corresponding to yolk granules (blue arrows). Abbreviations: Ld = lipid droplet, N = nucleus, Nu = nucleoli

of the theca cells contained electron dense masses (Fig. 1C), which correspond to small blocks of heterochromatin and a single small nucleolus in the nucleus.

With the progress of oogenesis, the size of late PG oocyte apparently increased reaching the diameter of 40.00±1.30 µm. The cytoplasm became less basophilic, showing the accumulation of cortical alveoli (Fig. 2A), along with the first formation of small lipid droplets in the peri-nuclear ooplasm (Figs. 2A-2B). The nudge bodies, mitochondria and ER cisterna were recognizable in the ooplasm, being more numerous than the previous oocyte stage (Figs. 2C-2D). The zona pellucida was thickened and had longer microvilli in association to granulosa cells (Fig. 1E). Several mitochondria and SER were observed in the granulosa cells increasing the thickness of the layer (Fig. 1E), but the arrangement of theca cells was similar to that of the previous stage.

Ultrastructure of oocyte and follicular complex in secondary growth phase (SG)

Secondary growth phase (SG) of *H. barbouri* was further divided into the early secondary growth step (Esg) and late secondary growth step (Lsg) (Figs. 3-4). The distinctive feature of the oocytes in the early secondary growth phase were characterized by its larger size than that of oocytes in the primary growth phase. The increase in oocyte size came at the same stage when moderately electron-dense small yolk granules progressively deposited close to the follicular complex (Fig. 3A). More specifically, multiple small coated vesicles were observed, indicating an intense transport in the membrane of zona pellucida (Figs. 3B-3C). In parallel to the well-developed microvilli, abundant finger-shaped cytoplasmic projections on the zona pellucida were noted with maximum structure thickness of 3 nm. Follicle cells, especially the granulosa cells, were well-recognized because of the increase in cell size to about 3.5 nm in diameter and apparent mitochondria and SER. Several electron-lucent materials or transport vesicles were scattered in the cytoplasm of granulosa cells (Fig. 3D), indicating the dynamics yolk transport.

The size of oocytes in the late secondary growth phase markedly increased (110.00±1.50 µm in diameter) during vitellogenesis. The coated vesicles coalesced with transport vesicles, forming small endosomes. Yolk granules also increased the size by the fusion of small vesicles at the peripheral ooplasm (Figs. 4A-4C). The yolk granule was heterogeneous, containing the small electron-dense granules in the matrix (Fig. 4C). Cortical alveoli and lipid droplets fused with the yolk granules (Figs. 4A-4B). The single-layered zona pellucida and granulosa cells were well-organized, becoming thicker during this secondary phase of growth (Fig. 4C). At higher magnification, the dilated SER and prominent mitochondria appeared in the granulosa cells (Fig. 4C).

Ultrastructure of atretic phase oocytes (Ao)

Atretic phase oocytes (Ao) were observed only in the secondary growth phase. The atretic phase were recognized by the presence of liquefactive yolk globules (Fig. 5A) as well as folding, fracturing and dissolution of follicular complex. The degeneration of SER became visible in the granulosa cells connected to the atretic oocytes (Fig. 5B). Numerous cytoplasmic vacuoles were also present in both granulosa and theca cells (Fig. 5B).

Ultrastructure of spermatocytes in H. barbouri testis

Seahorse *H. barbouri* testis was composed of the germinal epithelium and a testicular wall enclosing a large central cavity or lumen (Fig. 6A). Closely packed dense fibrous connective tissues was apparent within the testicular wall (Fig. 6A). Within the basal lamina, two types of cells: spermatogenic cells and Sertoli cells constitutes the germinal epithelium (Fig. 6B). Sertoli cells had an elongated shape spanning from the basal lamina to the lumen and a thick layer of Sertoli cells was decorated with scattered spermatogenic cells (Fig. 6A). Electron micrograph of the Sertoli cells identified the oval nucleus with small clumped heterochromatin surrounded by the slightly electron-dense cytoplasm (Fig. 6B).

The spermatogonia and the spermatocytes were easily recognizable and distributed throughout the testis (Fig. 6C).

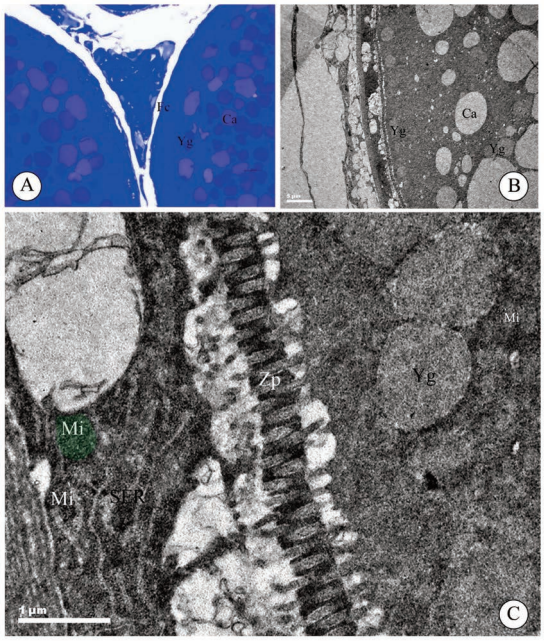

Fig. 4. Light microscope (A) and electron microscope (B-C) images of late secondary growth step oocytes of *Hippocampus barbouri*. A: The great development of follicular complex (Fc) was found. Yolk granules (Yg) and cortical alveoli (Ca) were present in the ooplasm. B-C: Large yolk granules (Yg) were formed and often located close to the follicular complex. High magnification images showed the great development of microvilli in the zona pellucida (Zp). At the same time, mitochondria (Mi) and smooth endoplasmic reticulum (SER) were clearly detected.

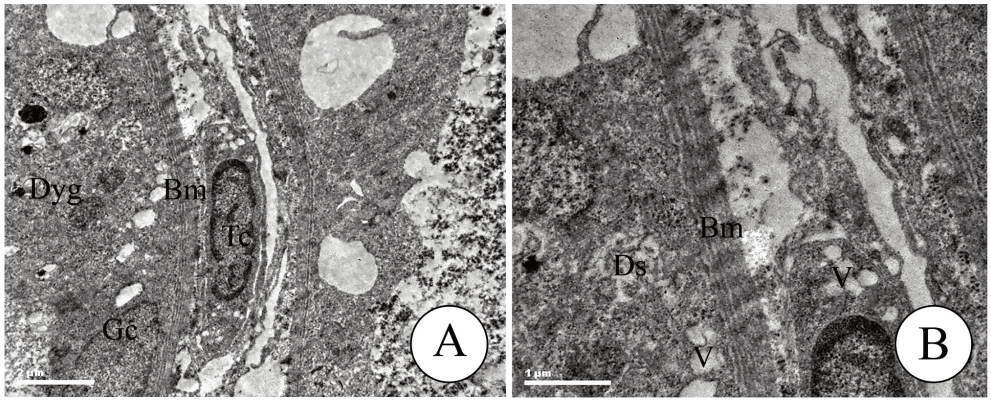

Fig. 5. Electron microscope images (A-B) of atretic oocytes during the secondary growth phase of *Hippocampus barbouri*. The degeneration of yolk granules (Dyg) was observed together with several vacuolated features in granulosa cells (Gc) and theca cells (Tc). The degenerated smooth endoplasmic reticulum (Ds) was detected in the granulosa cells. Abbreviations: Bm = basement membrane, V = Vacuoles.

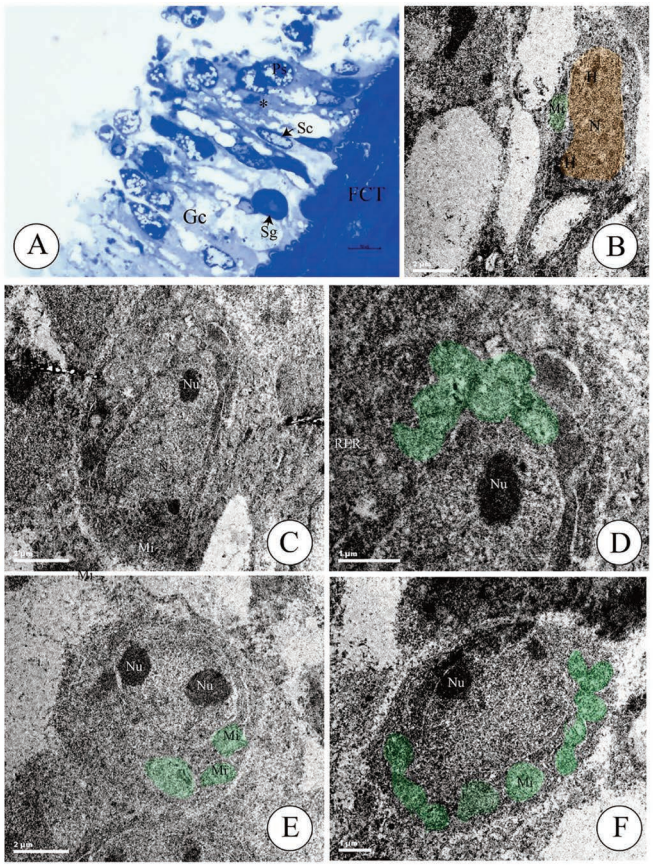

Fig. 6. Light microscope (A) and electron microscope (B-F) of male germ cells of *Hippocampus barbouri*. A: Germinal epithelium (Gc) was surrounded by the fibrous connective tissue (FCT). Several cell types including Sertoli cells (Sc), spermatogonia (Sg) and primary spermatocytes (Ps) were observed. The cytoplasm (asterisk) of Sertoli cells support the primary spermatocytes (Ps). B: Elongated Sertoli cells had mitochondria (Mi) and a spherical nucleus containing the prominent heterochromatin (H). C-D: Spherical spermatogonia had a single nucleolus (Nu) in the nucleus (N). The accumulation of mitochondria (Mi) and rough endoplasmic reticulum (RER) were the prominent. E-F: The oval primary spermatocytes containing one or two nucleoli (Nu). Several mitochondria (Mi) were observed in the cytoplasm.

The spermatogonia with the spherical shape were widely found near the testicular wall (Figs. 6A, 6C). The nucleus containing a single nucleolus was apparent in the spermatogonia (Figs. 6C-6D). The well-developed mitochondria and RER were clearly observed in the cytoplasm (Fig. 6D). Spermatocytes had an oval shape, in which the oval nucleus contained a few nucleoli (Figs. 6E-6F). The prominent mitochondria were continuously developed (Figs. 6E-6F).

Discussion

In the present study, characterization of gonadal tissue structures was reported in both sexes of zebra-snout *H. erectus*. For successful breeding program, precise determination of sex and reproductive status of the aquaculture seahorse can be achieved by using data on its ultrastructure of the gonads (Nur *et al*., 2016; Senarat *et al*., 2018). Observation from this study showed that the oogenic stages from primary growth phase to the secondary phase take place in the ovary of the seahorse at 30-31 days after birth, consistently with what shown in Kamnurdnin (2017). This time period of sample collection is considered as the onset of the early adult stage. In addition, the present study demonstrated that spermatozoa with flagellate morphology was absent in the testicular parenchyma of the male seahorse at the same age of collect-

ing ovaries, indicating delay of male maturity. This shift in the reproductive development can be influenced by several factors from aquaculture conditions such as nutritional status and temperature. Further examination of the reared seahorses from different time periods covering all seasons and samples from other aquaculture system will unravel the truth behind this prolonged testis development.

The oogenic ultrastructure of seahorses has been described in *H. erectus* (Wallace and Selman, 1990; Selman *et al*., 1991). The present study reported another aspect of ultrastructural features of the oocytes for *H. barbouri* by covering detail of cellular structures linking the oocyte to other ovarian follicular cells. Furthermore, early secreted zona pellucida in the early primary growth phase was embedded with numerous microvilli of the granulosa cells. The microvilli became well-developed and apparent as a thick layer in the late secondary growth phase. Emergence of microvilli at the early and late phases are closely related to the stage when vitellogenin expression is upregulated to produce yolk nutrients. Similar observations have been reported in other marine teleost fishes such as *H. erectus* (Wallace and Selman, 1990; Selman *et al*., 1991), *Pagrus major* (Matsuyama *et al*., 1991), *Chionodraco hamatus* (Baldacci *et al*., 2001), *Rastrelliger brachysoma* (Senarat *et al*., 2017) and *Kareius bicoloratus* (Jun *et al*., 2018). These elaborate processes are normally regulated by hypophyseal hormones via the hypothalamic-pituitary-gonadal axis in fish (Selman and Wallace, 1986; Selman *et al*., 1988). The electrodense material is transported from the granulosa cells through pores in the zona pellucida (Selman and Wallace, 1983). The uptake of vitellogenin-derived yolk protein from the granulosa cells to the ooplasm is assisted by mechanism of endocytosis. The yolk protein then translocated to the nascent yolk granules, as confirmed by exploration and other investigations (Selman and Wallace, 1983, 1986; Yon and Akbulut, 2012; Jun *et al*., 2018). It is the same process that has been observed in other fish (Selman and Wallace, 1983, 1986; Abascal and Medina, 2005) such as *Cyprinodon variegatus* (Selman and Wallace, 1986) and *Fundulus heteroclitus* (Selman and Wallace, 1983).

Two major follicle cell layers (granulosa cells and special thecal cells) are capable of producing ovarian steroid hormones (Shackley and King, 1977; Nagahama *et al*., 1982; Fostier *et al*., 1983; Nagahama 1983) as confirmed in several different orders of fishes such as Labriformes (Santos-Silva *et al*., 2015), Perciformes (Grier *et al*., 2017) and Siluriformes (Rodrigues-Filho *et al*., 2017). This study showed that the prominent changes in the granulosa cells takes place at the late secondary growth phase, when smooth endoplasmic reticulum (SER) appears prominent and number of mitochondria per cell increases dramatically. This suggests that the granulosa cells might be the major site of steroid synthesis in *H. barbouri*. This is consistent with a report by Voorhis (1999) who postulated that the granulosa cells play roles in the production of estrogen, whereas the androgen production was concentrated in the theca cells, although several documents suggest that the activity of the granulosa and theca cells are transformed during primary oocyte to oocyte maturation in the ovary of some teleost including *O. kisutch* (Nagahama *et al*., 1978), S. leucomaenis (Kagawa *et al*., 1981), *Oncorhynchus rhodurus* (Kagawa, 1985) and *Chirostoma humboldtianum* (Cárdenas *et al*., 2008). It would be thus interesting to further investigate on granulosa activity in the follicular complex. Indeed, an in vitro experiment using isolated follicle cell layers showed that the granulosa cells are steroidogenic responsible for the production of estradiol-17β during vitellogenesis (Young *et al*., 1983, 1986; Kanamori *et al*., 1988).

To the best of the authors' knowledge, very limited information is available for the spermatogenesis of seahorses. The spermatogenesis has been described in *H. guttulatus*, but ultrastructures are only shown for mature sperms (Piras *et al*., 2015). The ultrastructure of spermatogonia and spermatocytes are firstly reported in the present study, while the oval spermatogium containing single nucleoli has been similarly found in other fishes (Lee *et al*., 2006; Kang *et al*., 2016; Senarat *et al*., 2018).

Conclusion

The ultrastructure of the ovarian follicular complex including zona pellucida, granulosa and theca cells of *H. barbouri* was described for the first time in this current study. Although both granulosa and theca cells have been proposed as the major site for steroid production in other fish, the granulosa cells are likely to be the main site of follicular steroid production in *H. barbouri*. Further studies involving Immunohistochemistry or gene expression of follicular cell in this seahorse would be useful for better understanding of the oogenesis on this species.

Conflict of interest

The authors declare that they have no conflict of interest.

References

Abascal, F.J., Medina, A., 2005. Ultrastructure of oogenesis in the bluefin tuna, *Thunnus thynnus*. Journal of Morphology 264, 149-160.

Baldacci, A., Taddei, A.R., Mazzini, M., Fausto, A.M., Buonocore, F., Scapigliti, G., 2001. Ultrastructure and proteins of the egg chorion of the Antarctic fish *Chionodraco hamatus* (Teleostei, Notothenioidei). Polar Biology 24, 417-421.

Cárdenas R., Chávez, M., González, J.L., Aley, P., Espinosa, J., Jiménez-García, L.F., 2008. Oocyte structure and ultrastructure in the Mexican silverside fish *Chirostoma humboldtianum* (Atheriniforme: Atherinopsidae). Revista de Biologia Tropical 56, 1371-1380.

Culling, C.F.A., 1974. Handbook of Histopathological and Histochemical Techniques: Including Museum Techniques. Oxford, England: Butterworth-Heinemann, p 726.

Fostier, A., Jalabert, B., Billard, R., Breton, B., Zohar, Y., 1983. The gonadal Sterids. In: Hoar, W.S., Randall, D.J., & Donaldson, E.M. (eds.), Fish Physiology. Volume IX, Academic Press: London, pp. 277-372.

Grier, H.J., 2012. Development of the follicle complex and oocyte staging in red drum, *Sciaenops ocellatus* Linnaeus, 1776 (Perciformes, Sciaenidae). Journal of Morphology 273, 801-829.

Grier, H.J., Neidig, C.L., Quagio-Grassiotto, I., 2017. Development and fate of the postovulatory follicle complex, postovulatory follicle, and observations on folliculogenesis and oocyte atresia in ovulated common snook, *Centropomus undecimalis* (Bloch, 1792). Journal of Morphology 278, 547–562.

International Union for Conservation of Nature, IUCN, 2002. The IUCN Seahorse, Pipefish and Seadragon Specialist Group, Institute for the Oceans and Fisheries, Vancouver, Canada.

Jun, J.C., Gang, H.W., Lee, K.Y., 2018. Ultrastructural studies on oocyte differentiation and vitellogenesis in the oocytes of female *Kareius bicoloratus* in Western Korea. Development and Reproduction 22, 213-223.

Kagawa, H., Takano, K., Nagahama, Y., 1981. Correlation of plasma estradiol-17a and progesterone levels with ultrastructure and histochemistry of ovarian follicles in the whitespotted char, *Salvelinus leucomaenis*. Cell and Tissue Research 218, 315-329.

Kagawa, H., 1985. Ultrastructure and histochemical observations regarding the ovarian follicles of amago salmon (*Oncorhynchus rhoduros*). Journal of University of Occupational and Environmental Health 7, 27-35.

Kamnurdnin, T., 2017. Effects of food on growth and gonadal development of seahorse *Hippocampus* sp. Master of Science Thesis, Chulalongkorn University, Faculty of Science, Bangkok, Thailand.

Kanamori, A., Adachi, S., Nagahama, Y., 1988. Developmental changes in steroidogenic responses of ovarian follicles of amago salmon (*Oncorhynchus rhodurus*) to chum salmon gonadotropin during oogenesis. General and Comparative Endocrinology 72, 13-24

Kang, H.W., Kim, S.H., Chung, J.S., 2016. Ultrastructural studies of germ cell development and the functions of leydig cells and sertoli cells associated with spermatogenesis in *Kareius bicoloratus* (Teleostei, Pleuronectiformes, Pleuronectidae). Development and Reproduction 20, 11–22.

Lee, T.H., Chiang, T.H., Huang, B.M., Wang, T.C., Yang, H.Y., 2006. Ultrastructure of spermatogenesis of the paradise fish, *Macropodus opercularis*. Taiwania International Journal of Biodiversity 51, 170-180.

Matsuyama, M., Nagahama, Y., Matsura, S., 1991. Observations on ovarian follicle ultrastructure in the marine teleost, *Pagrus major* during vitellogenesis and oocyte maturation. Aquaculture 92, 67-82.

Nagahama. Y., Clarke, W.C., Hoar, W.S., 1978. Ultrastructure of putative steroid-producing cells in the gonads of coho (*Oncorhynchus kisutch*) and pink salmon (*Oncorhyzchzu gorhuscha*). Canadian Journal of Zoology 56, 2508-2519.

Nagahama, Y., Kagawa, H., Young, G., 1982. Cellular sources of sex steroids in teleost gonad. Canadian Journal of Fisheries and Aquatic Sciences 39, 56-64.

Nagahama, Y., 1983. The functional morphology of teleost gonads. In: Fish Physiology, volume IX A. Reproduction, endocrine tissues and hormones, (W.S. Hoar, D.J. Randall & E.M. Donaldson, eds.). Academic Press: New York, U.S.A., pp. 223-276.

Nur F.A.H., Christianus, A., Muta Harah, Z., Ching, F.F., Shapawi, R., Saad, C.R., Senoo, S., 2016. Reproductive performance of seahorse, *Hippocampus barbouri* (Jordan and Richardson 1908) in control condition. Journal of Survey in Fisheries Sciences 2, 17-33.

Nyuji, M., Kitano, H., Shimizu, A., Lee, J.M., Kusakabe, T., Yamaguchi, A., Matsuyama, M., 2013. Characterization, localization, and stage-dependent gene expression of gonadotropin receptors in chub mackerel (*Scomber japonicus*) ovarian follicles. Biology of Reproduction 88, 148, 1-14.

Pirast, F., Biagi, F., Taddei, A.R., Fausto, A.M., Farina, V., Zedda, M., Floris, A., Franzoi, P., Carcupino, M., 2015. Male gonads morphology, spermatogenesis and sperm ultrastructure of the seahorse *Hippocampus guttulatus* (Syngnathidae). Acta Zoologica 97, 325–333.

Rodrigues-Filho, J.A., Honji, R.M., Mello, P.H., Borella, M.I., Hilsdorf, A.W.S., Moreira, R.G., 2017. Reproductive biology of *Pseudotocinclus tietensis* (Siluriformes: Loricariidae: Hypoptopomatinae), a threatened fish species. International Journal of Aquatic Biology 5, 218–227.

Rowden, G., Lewis, M.G., 1974. Experience with a three-hour electron microscopy biopsy service. Journal of Clinical Pathology 27, 505-510.

Santos-Silva, A.P., Siqueira-Silva, D.H., Ninhaus-Silveira, A., Veríssimo-Silveira, R., 2015. Oogenesis in *Laetacara araguaiae* (Ottoni and Costa, 2009) (Labriformes: Cichlidae). Zygote 24, 502–510.

Selman, K., Wallace, R.A., 1983. Oogenesis in *Fundulus heteroclitus*. III. Vitellogenesis. Journal of Experimental Zoology 226, 441-457.

Selman, K., Wallace, R.A., 1986. Gametogenesis in *Fundulus heteroclitus*. American Zoologist 26, 173-192.

Selman, K., Wallace, R.A., Barr, V., 1988. Oogenesis in *Fundulus heteroclitus*. V. The relationship of yolk vesicles and cortical alveoli. Journal of Experimental Zoology 246, 42-56.

Selman, K., Wallace, R.A., Player, D., 1991. Ovary of the seahorse, *Hippocampus erectus*. Journal of Morphology 209, 285–304.

Senarat, S., Kettretad, J., Jiraungkoorskul, W., 2017. Structure and ultrastructure of oogenic stage in short mackerel *Rastrelliger brachysoma* (Teleostei: Scombidae). Journal of Morphological Science 34, 23-30.

Senarat, S., Kettretad, J., Jiraungkoorskul, W., 2018. Testicular structure and spermatogenesis of short mackerel, *Rastrelliger brachysoma* (Bleeker, 1851) in The Upper Gulf of Thailand. Asia-Pacific Journal of Molecular Biology and Biotechnology 26, 30-43.

Shackley, S.E., King, P.E., 1977. Oogenesis in a marine teleost, Blennius pholis L. Cell and Tissue Research 181, 105-128.

Vincent A.C.J., 1996. The International Trade in Seahorses. A Traffic Network Report, Traffic International: Cambridge, U.K., 163p.

Voorhis, B.J.V., 1999. Follicular Steroidogenesis. Encyclopedia of Reproduction. volume 2. Academic Press: Massachusetts, U.S.A., pp. 389-395.

Wallace, R.A., Selman, K., 1990. Ultrastructural aspects of oogenesis and oocyte growth in fish and amphibians. Journal of Electron Microscopy Technique 16, 175–201.

Yon, N.D., Akbulut, C., 2012. Electron and light microscopic investigations of follicular epithelium in vitellogenic oocyte of zebrafish (*Danio rerio*). Pakistan Journal of Zoology 44, 1581-1586.

Young, G., Ueda, H., Nagahama, Y., 1983. Estradiol-17 alpha, 20 beta-dihydroxy-4-pregnen-3-one production by isolated ovarian follicle of amago salmon (*Oncorhynchus rhodurus*) in reponse to mammalian pituitary an placental hormones and salmon gonadotropin. General and Comparative Endocrinology 52, 329-335.

Young, G., Adachai, S., Nagahama, Y., 1986. Role of ovarian thecal and granulosa layers in gonadotropin-induced synthesis of a salmonid maturation-inducing substance (17 alpha, 20 beta-dihydroxy-4-pregnen-3-one). Developmental Biology 118, 1-8.